

Differential Pair Distribution Function Study of the Structure of Arsenate Adsorbed on Nanocrystalline γ -Alumina

Wei Li,^{*,†,⊥} Richard Harrington,^{*,†,‡} Yuanzhi Tang,^{*,†,¶} James D. Kubicki,[§] Masoud Aryanpour,^{§,||} Richard J. Reeder,[†] John B. Parise,^{†,‡} and Brian L. Phillips[†]

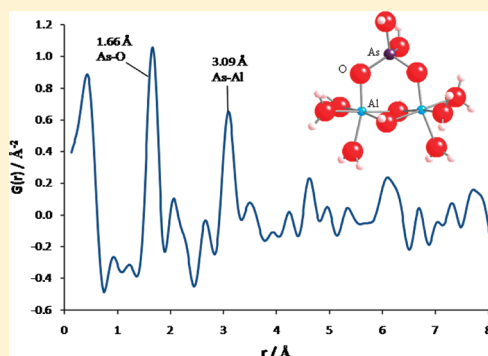
[†]Department of Geosciences and Center for Environmental Molecular Science, Stony Brook University, Stony Brook, New York 11794-2100, United States

[‡]Department of Chemistry, Stony Brook University, Stony Brook, New York 11794-3400, United States

[§]Department of Geosciences, Pennsylvania State University, University Park, Pennsylvania 16802, United States

S Supporting Information

ABSTRACT: Structural information is important for understanding surface adsorption mechanisms of contaminants on metal (hydr)oxides. In this work, a novel technique was employed to study the interfacial structure of arsenate oxyanions adsorbed on γ -alumina nanoparticles, namely, differential pair distribution function (d-PDF) analysis of synchrotron X-ray total scattering. The d-PDF is the difference of properly normalized PDFs obtained for samples with and without arsenate adsorbed, otherwise identically prepared. The real space pattern contains information on atomic pair correlations between adsorbed arsenate and the atoms on γ -alumina surface (Al, O, etc.). PDF results on the arsenate adsorption sample on γ -alumina prepared at 1 mM As concentration and pH 5 revealed two peaks at 1.66 Å and 3.09 Å, corresponding to As–O and As–Al atomic pair correlations. This observation is consistent with those measured by extended X-ray absorption fine structure (EXAFS) spectroscopy, which suggests a first shell of As–O at 1.69 ± 0.01 Å with a coordination number of ~ 4 and a second shell of As–Al at $\sim 3.13 \pm 0.04$ Å with a coordination number of ~ 2 . These results are in agreement with a bidentate binuclear coordination environment to the octahedral Al of γ -alumina as predicted by density functional theory (DFT) calculation.



INTRODUCTION

Surface adsorption reactions occurring at mineral/water interface are of great importance for water treatment, nutrient management, and soil decontamination.^{1,2} To achieve comprehensive understanding of the adsorption mechanisms of aqueous solutes to solid surfaces, research tools that provide detailed structural information of species on solid surfaces are essential. In the past thirty years, successful applications of extended X-ray absorption fine structure (EXAFS) spectroscopy to inorganic ion adsorption studies have demonstrated the power of spectroscopic techniques in providing the details of interfacial solutes adsorption at the atomic to molecular scale.³ However, EXAFS has some limitation, for example, in studying the systems containing light elements (i.e., P, Al, etc.). Therefore, the development of new experimental techniques that complement EXAFS for probing surface structures is an active area of research.

X-ray diffraction (XRD) has been used to determine the atomic-scale structure of materials for a century by analyzing Bragg peaks arising due to translation symmetry in crystals. However, this traditional method breaks down when one attempts to study the structure of species with shorter length scales.^{4–7} One way around this is to take the Fourier transform of the total scattering pattern (both Bragg and diffuse scattering), correctly

normalized, to produce the pair distribution function (PDF). The PDF shows the probability of finding an atom at a given distance r from another atom.^{8,9} This technique does not require long-range order and, therefore, is ideal for the study of liquids, amorphous solids, and nanoparticles. Recently, with the high flux and short wavelength X-rays available at third generation synchrotron sources and the use of fast read out area detectors that are able to simultaneously collect the total scattering pattern, differential pair distribution function (d-PDF) analysis becomes practical for a wide range of systems. This technique involves the subtraction of a reference PDF of the pristine sample from the PDF of the sample after reaction, leaving only the difference between two samples.^{10–14} Recently, this technique has been applied to the structures of adsorbates on the surface of nanomaterials.^{15,16} The correlations arising from the host–guest relationship are obtained by subtracting the atomic correlations of the bulk material (Host) from the adsorption material (Host + Guest) as shown in Scheme 1. Harrington et al.,¹⁶ using high

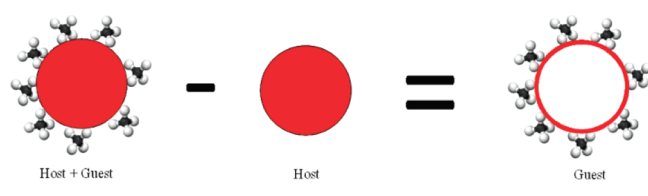
Received: March 4, 2011

Accepted: October 11, 2011

Revised: September 10, 2011

Published: October 11, 2011

Scheme 1. Illustration of Differential Pair Distribution Function (d-PDF)



energy synchrotron radiation, investigated the structure of arsenate oxyanion adsorbed on the surface of 2-line ferrihydrite, a naturally occurring iron oxyhydroxide with particles typically 2–3 nm in size.^{17,18} Using the differential PDF technique, several correlations were observed, including an As–Fe correlation of 3.26 Å. This As–Fe correlation has a distance similar to that obtained from As K-edge EXAFS,^{19,20} which suggested a bridging bidentate binuclear surface structure of As absorbed on 2-line ferrihydrite. Further correlations were also observed in the d-PDF, corresponding to the correlations between the adsorbed As and the oxygen atoms from within the 2-line ferrihydrite particle, which were not previously observed using EXAFS.

In this work, we expanded the application of d-PDF technique to arsenate adsorption on γ -alumina (γ -Al₂O₃). γ -Alumina is an important industrial nanomaterial and is extensively used in geochemistry and environmental chemistry research as a model compound for studying the surface reactivity of Al (hydr)oxides and clays, as well as for the exploration of the mechanisms of heavy metals/metalloids adsorption on metal oxides.^{21–25} Compared to 2-line ferrihydrite (2 nm in size), the size of γ -alumina is larger (10–20 nm); consequently, it is likely that there will be less surface interactions for the same volume illuminated by the X-ray beam. Another challenge for this system is the much weaker X-ray scattering property of Al atoms due to its lower Z compared to Fe. If d-PDF can successfully determine the arsenate bonding structure on γ -alumina, this technique can be applied to other engineered nanomaterials (e.g., nano-TiO₂). The purpose of this study is to apply the novel d-PDF technique to study the mechanism(s) of arsenate adsorption on γ -alumina and to compare the results with other experimental (X-ray absorption) and theoretical (density function theory, DFT) techniques.

EXPERIMENTAL SECTION

Preparation of Adsorption Samples. Adsorption samples were prepared by adding 0.25 g of dry γ -alumina powder (Aluminum Oxide C, Degussa) to 50 mL of vigorously stirring solution containing 0.01 M NaCl background electrolyte at pH 5. We chose pH 5 because at this pH As exists almost 100% as H₂AsO₄[−] (aq). The pH was carefully maintained using automatic titrators (Metrohm STAT 718) with 0.1 M HCl and 0.1 M NaOH. The adsorption isotherm experiments were carried out at pH 5 with initial As concentration of 0.1–10 mM. A short reaction time (15 min) was chosen to avoid precipitation. After reaction, the samples were centrifuged (10 000g, 15 min) to separate the solid and solution. The supernatants were analyzed for arsenate concentration using directly coupled plasma-atomic emission spectrometry (DCP-AES).

Three wet paste samples with initial arsenate concentrations of 0.1, 0.4, and 1 mM were prepared for EXAFS measurement. One air-dried sample with 1 mM initial arsenate concentration was prepared for both EXAFS and d-PDF studies. For d-PDF, a

control sample was prepared with identical treatment but without adding arsenate to the solution.

Differential PDF. Powder diffraction experiments were carried out at beamline 11-ID-B at the Advanced Photon Source (APS; Argonne National Laboratory, Argonne, IL) using monochromatic X-rays with energy of ~ 90 keV ($\lambda = 0.12702$ Å) in transmission mode with samples loaded in polyamide (kapton) capillaries. The diffraction pattern was collected using an amorphous Si detector manufactured by General Electric.^{26,27} The beamline was calibrated using a CeO₂ standard (NIST 674b). The data was converted from 2D to 1D using the program Fit2D.²⁸ Using the program PDFgetX2,²⁹ PDFs were generated by Fourier transformation of the total structure function, $S(Q)$, with a Q_{max} of 24 Å^{−1}, after being corrected for background scattering, Compton scattering, and oblique incidence as described previously.²⁶ Differential PDFs were obtained by subtraction of a reference PDF (γ -alumina with no arsenate loading) from a PDF of arsenate-sorbed γ -alumina in real space using Microsoft Excel. The control was multiplied by an appropriate constant to ensure that the scale of each PDF was the same. Interatomic distances were quantified by fitting the peaks with a Gaussian function.

EXAFS Spectroscopy. Extended X-ray absorption fine structure (EXAFS) spectroscopy data were collected on the arsenate sorption samples and the reference compounds, a 10 mM As(V) solution and the mineral mansfieldite (AsAlO₄·2H₂O). Details of the data collection and analysis are provided in the Supporting Information.

Quantum Chemical Calculations. The structures of adsorbed arsenate anions on the (010) and (001) surfaces of γ -alumina were calculated using quantum chemical calculation. Details on the cluster construction can be found in Supporting Information.

RESULTS

Arsenate Adsorption on γ -Alumina. Systematic characterization of γ -alumina sorbent by powder X-ray diffraction, SEM, TEM, and ²⁷Al NMR are provided in Figures S1–S4, Supporting Information. These results are consistent with previous studies of similar material³⁰ and indicate no impurity. Arsenate adsorption isotherm was carried out within the range of 0.1 to 1 mM initial arsenate concentration (Figure 1). Over this range, the surface coverage increased from 19.1 $\mu\text{mol g}^{-1}$ (0.13 molecules nm^{−2}) to 187.8 $\mu\text{mol g}^{-1}$ (1.25 molecules nm^{−2}). A Langmuir isotherm equation, $Q = (Q_{\text{m}}KC)/(1 + KC)$, was used to fit the adsorption isotherm, where Q is the amount of adsorbed arsenate ($\mu\text{mol g}^{-1}$), C is the equilibrium arsenate concentration (μM), Q_{m} is the maximum adsorption amount, and K is the equilibrium constant for the sorption reaction. The fitting results ($R^2 = 0.97$) give the Q_{m} value as 319.2 $\mu\text{mol g}^{-1}$ and K as 0.037. With higher arsenate concentration (up to 10 mM), an adsorption capacity of ca. 370 $\mu\text{mol g}^{-1}$ can be achieved, but the extended isotherm (Figure 1 inset) can not be well fitted using a one-site Langmuir equation. Such sorption capacity of γ -alumina is comparable to several other reported adsorbents,^{31,32} with the comparison provided in Table S1, Supporting Information. The sample prepared for d-PDF investigation has an arsenate surface loading of 187.8 $\mu\text{mol g}^{-1}$, much lower than the maximum adsorption capacity. Given the short reaction time and low arsenate concentration,³³ we consider it unlikely that any significant

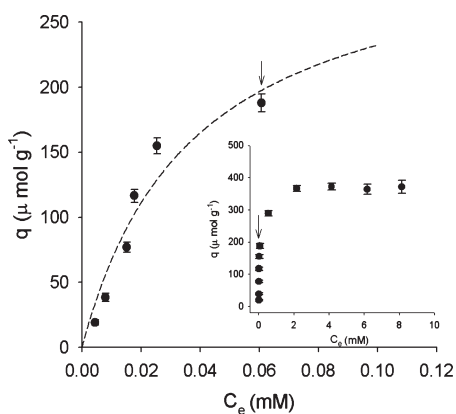


Figure 1. Adsorption isotherm of arsenate on γ -alumina at pH 5. Inset shows extend adsorption isotherm to higher concentration range. Arrow denotes the sample used for d-PDF analysis.

amount of aluminum arsenate precipitates would form during the sorption experiments.

Differential PDF. The PDFs of bulk γ -alumina, γ -alumina with arsenate adsorbed on the surface, and the difference between them (the d-PDF) are shown in Figure 2a. The d-PDF comprises only correlations containing arsenate, as the other correlations are present in both the loaded sample and the control and are consequently subtracted out. The difference between the two PDFs is very small (Figure 2a); consequently, the d-PDF is noisy. However, two peaks at 1.66 and 3.09 Å are clearly observed in Figure 2b. The first correlation at 1.66 Å is in good agreement of the As–O distance (1.68 Å) in most arsenate minerals (e.g., scorodite²⁰), and the second peak at 3.09 Å is assigned as an As–Al atomic pair correlation, the next logical correlation in this system. The value of r is similar to the As–Al distance (3.11 ± 0.03 Å) determined by Arai et al.²² using EXAFS which suggests the formation of inner-sphere bidentate binuclear complexes.

Figure S5 in the Supporting Information shows four d-PDFs calculated using different values of Q_{\max} in the Fourier transform. The two aforementioned peaks remain at the same value of r no matter what value of Q_{\max} is used; other peaks in the d-PDF calculated using a Q_{\max} of 24 \AA^{-1} (Figure S5, Supporting Information) are not present at the same r in the d-PDFs calculated using lower values of Q_{\max} , indicative of noise. Owing to the low signal-to-noise ratio, we cannot assign peaks at r values greater than 4 Å, even though such assignments were possible in a similar study of ferrihydrite.¹⁶ This is attributed to the higher electron density of Fe compared to Al. All features beyond 4 Å are well within noise according to the spectra processed using different Q_{\max} for Fourier transform (Figure S5, Supporting Information).

Arsenic K-Edge EXAFS. For comparison with the d-PDF results, we obtained As K-edge EXAFS for the same samples as well as the two model compounds (Figure 3a). The spectra of all samples are dominated by a strong oscillation from the backscattering of the first oxygen shell, leading to a subtle difference showing only at k ranges of $\sim 11\text{--}13 \text{ \AA}^{-1}$. The corresponding Fourier transforms (Figure 3b) for all samples are dominated by the contribution from the first oxygen shell, which is best fit with ~ 4 O atoms at 1.69 ± 0.01 Å (Table S2, Supporting Information). Compared to the arsenate solution sample, all adsorption samples also show additional peaks at 2.5–3 Å in R space, which are best fit with ~ 2 Al atoms at 3.13 ± 0.04 Å,

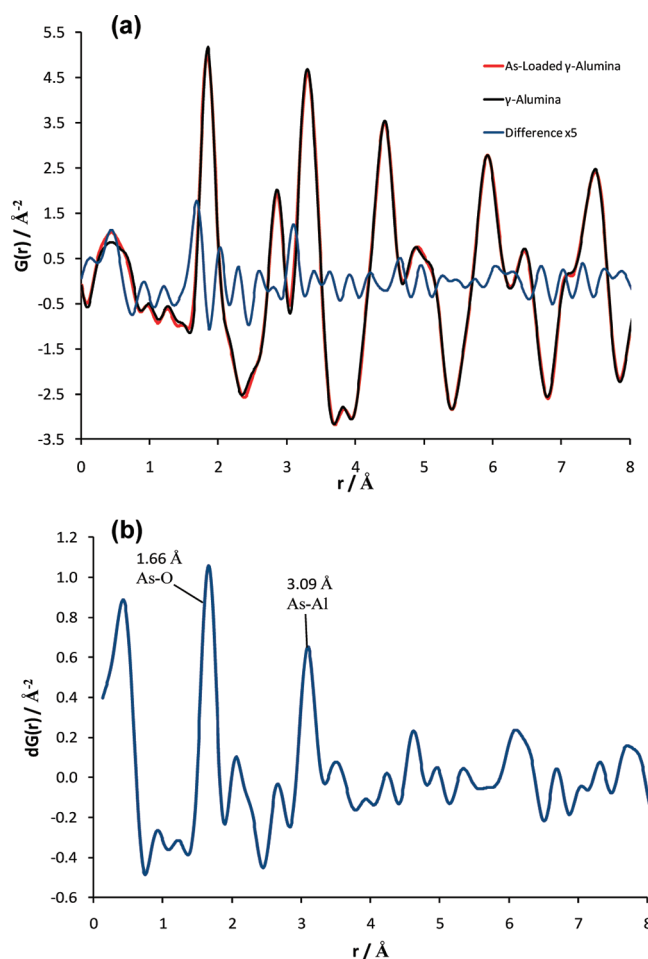


Figure 2. (a) The PDFs of γ -alumina (black line), γ -alumina loaded with As (red line), and the difference between these two spectra (multiplied 5 times for clarity; shown in blue line); (b) the smoothed d-PDF of arsenate adsorbed on γ -alumina, r -averaged over normalization ripples.

similar to the results of Arai et al.²² However, due to the weak backscattering property of Al atoms, the second shell is not well resolved;^{22,32} therefore, the Debye–Waller factor was fixed at 0.006 to reduce the number of free parameters. This value is determined from fitting of the reference compound mansfieldite. No significant differences are observed between results obtained for samples analyzed as wet pastes and dried powders.

Quantum Chemical Calculation. As previous studies^{22,25} only consider octahedral Al to interpret arsenate sorption mechanism, we conducted quantum chemical calculations to model the arsenate binding to γ -alumina (010) and (001) surfaces such that both tetrahedral and octahedral Al are taken into account. Tetrahedral Al on the (001) surface and octahedral Al on the (010) surface of γ -alumina were constructed as suggested by Pinto et al.,³⁴ and arsenate was bonded to both types of sites. Only the monodentate mononuclear structure was considered for As atoms connected to tetrahedral Al sites (Figure 4a) because a bidentate structure (i.e., edge-sharing) is not likely. Both a monodentate (Figure 4b) and a bidentate binuclear structure (Figure 4c) were constructed for arsenate on the (010) surface, and a bidentate mononuclear structure was excluded due to the instability of this structure as previously suggested.^{20,35} An H_2AsO_4^- group

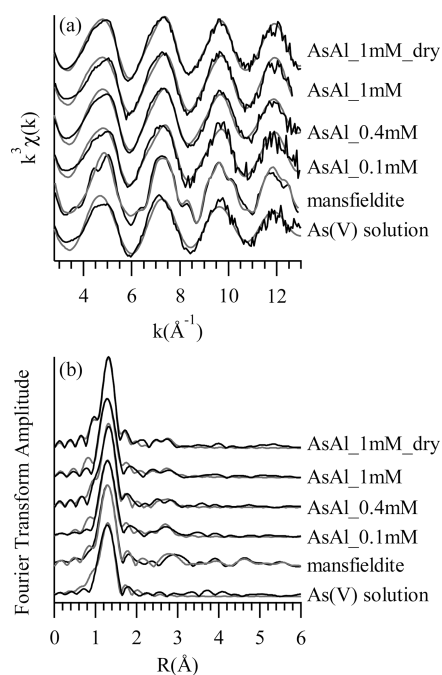


Figure 3. (a) κ^3 -weighted EXAFS data of sorption samples and the reference compounds, As(V) solution, and mansfieldite; (b) corresponding Fourier transforms (not corrected for phase shift) showing both raw (black lines) and fitted spectra (gray lines).

on γ -alumina was simulated in an attempt to mimic the reaction occurring at pH 5. The DFT calculations suggest the interatomic distances between As and Al for bidentate binuclear structures are 3.09 and 3.23 Å. This is distinct from the two monodentate models (Figure 4a,b), which give similar As–Al distances (3.36 and 3.37 Å, respectively).

DISCUSSION

Arsenate Bonding Structure on γ -Alumina. The interatomic distances of $d_{(\text{As}-\text{O})}$ and $d_{(\text{As}-\text{Al})}$ obtained by d-PDF, EXAFS, and DFT are compared in Table 1. The $d_{(\text{As}-\text{O})}$ determined by d-PDF is 1.66 Å, in good agreement with arsenate tetrahedron^{15,20,22} and EXAFS analysis (1.69 ± 0.01 Å). Unfortunately, it is difficult for d-PDF to provide coordination numbers, especially in a system with weak backscatterer (O and Al atoms). In principle, analyzing the peak intensities for As–O and As–Al correlations in the d-PDF could yield approximate coordination numbers. However, such analysis is prohibited due to the low signal-to-noise ratio. On the other hand, analysis of the EXAFS data suffers from the weak back scattering properties of Al atoms, resulting in large errors for the As–Al coordination number ($\pm 40\%$). In such a situation, DFT calculations are useful to help the interpretation of d-PDF and EXAFS data. The predicted As–O distances in all DFT calculated clusters (i.e., 1.68–1.79 Å) are in good agreement with those predicted by Ladeira et al.³⁵ and Sherman and Randall,²⁰ which are also similar to those experimentally measured by d-PDF and EXAFS. The calculated As–Al distances for monodentate surface complexes connecting to either tetrahedral Al or octahedral Al are similar (~ 3.36 Å) and are much larger than those measured by d-PDF and EXAFS (~ 3.09 and 3.13 Å, respectively). In contrast, the bidentate structure (Figure 4c) gives two $d_{(\text{As}-\text{Al})}$ as 3.09 and

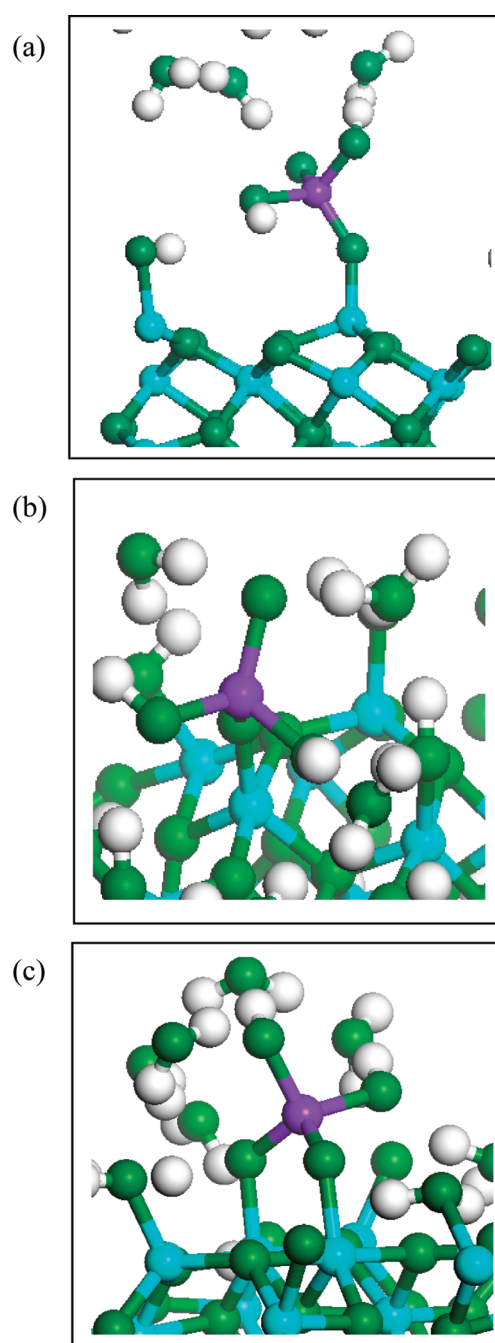
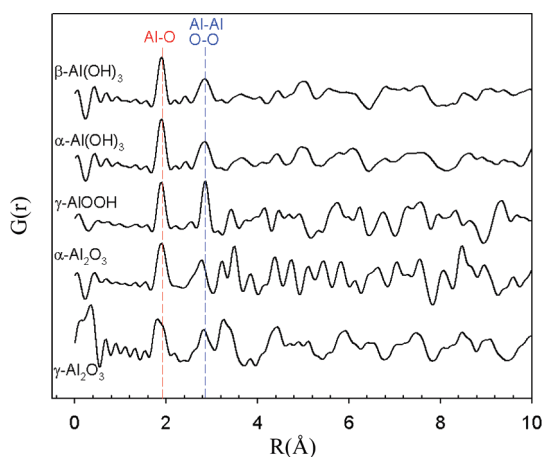


Figure 4. Optimized geometries of arsenate/alumina clusters calculated using density functional theory: (a) Biprotonated monodentate As coordinated with tetrahedral Al on (001) face; (b) biprotonated monodentate As coordinated with octahedral Al on (010) face; (c) biprotonated bidentate As coordinated with octahedral Al on (010) face. White balls represent H atoms, green for O, light blue for Al, and purple for As. Only a few atoms are shown for clarity. Graphics created with Materials Studio 5.5 (Accelrys Inc., San Diego CA).

3.23 Å. The averaged value (3.16 Å) is close to that from the EXAFS and d-PDF values (Table 1). The small differences between the averaged $d_{(\text{As}-\text{Al})}$ obtained by DFT and those from EXAFS/d-PDF are possibly due to the disordered nature of γ -alumina.^{32,33} In addition, the second peak at 3.09 Å in the d-PDF (Figure 2b) is as sharp as the first peak (As–O correlation). This observation further implies that a monodentate structure is unlikely,

Table 1. Comparison of the Interatomic Distances Obtained from Differential PDF, EXAFS, and DFT Calculation

method	sample/model	interatomic distance	
		As–O (Å)	As–Al (Å)
d-PDF	1 mM, pH 5, dry	1.66	3.09
EXAFS	1 mM, pH 5, dry	1.69	3.13
	0.1 mM, pH 5, wet	1.69	3.12
	0.4 mM, pH 5, wet	1.69	3.15
	1 mM, pH 5, wet	1.69	3.12
	mono-Al[4]-(001)	1.79, 1.70, 1.78, 1.68	3.368
	DFT	mono-Al[6]-(010)	1.70, 1.69, 1.79, 1.73
	bi-Al[6]-(010)	1.69, 1.73, 1.77, 1.72	3.09, 3.23

**Figure 5.** Pair distribution functions of γ -alumina (γ - Al_2O_3), corundum (α - Al_2O_3), boehmite (γ - AlOOH), gibbsite (α - $\text{Al}(\text{OH})_3$), and bayerite (β - $\text{Al}(\text{OH})_3$).

since the As–O–Al bonds in a monodentate surface complex would have a large degree of freedom (i.e., rotation about the As–O–Al linkage) and lead to a large thermal factor and a broadening of this peak.¹⁶ It is worth noting that the average As–Al distance (3.12 Å) measured for As adsorbed on γ -alumina is slightly shorter than those for As adsorbed on gibbsite³⁵ and other Al-rich minerals³⁶ (3.19–3.23 Å). This is possibly due to the differences in local structures among these Al (hydr)oxides as illustrated in the PDFs (Figure 5). The three samples with varied initial As concentrations have similar EXAFS features and fitting results, we therefore propose that arsenate forms bidentate binuclear structure from throughout the concentration range examined, i.e., from low surface loading (0.130 molecules per nm^{-2} or $0.216 \mu\text{mol m}^{-2}$) to high surface loading (1.25 molecules nm^{-2} or $2.08 \mu\text{mol m}^{-2}$).

Comparison of d-PDF and EXAFS. In this work, similar interatomic distances were obtained from d-PDF and EXAFS measurement, providing strong support for our interpretation of arsenate bonding structure. As in inelastic X-ray spectroscopy, EXAFS suffers from signal loss with the increase of incident X-ray energy,³⁷ resulting in a significant signal decay as the interatomic distance increases in the radial structural function (RDF), whereas PDF, intrinsically as a diffraction technique, is capable of avoiding such signal loss. This is one reason that the As–Al correlation is more evident in the d-PDF spectra than that in EXAFS analysis.

The peaks in PDF have a full width at half-maximum (fwhm) of $0.22\text{--}0.24 \text{ \AA}^{-1}$, which are intrinsically much sharper than those in the RDF of EXAFS spectra (FMHW of $0.4\text{--}0.5 \text{ \AA}^{-1}$), such that the interatomic distances can be obtained straightforwardly. The drawback of d-PDF, especially at this developing stage, is the difficulty in estimating the errors associated with interatomic distances and coordination numbers, whereas EXAFS is a well-developed method that has systematic procedures for data analysis. Furthermore, EXAFS is exclusively sensitive to local structure,³⁷ whereas d-PDF is sensitive to both local and intermediate structure.^{4–6} In most cases for interfacial studies, EXAFS can provide information for the first two shells (atomic correlations) in its RDF, with r less than 5 Å.

Previous d-PDF study¹⁶ of arsenate adsorbed on 2-line ferrihydrite showed that atomic correlations can be observed to higher r (up to $\sim 7 \text{ \AA}$). This present study is less favorable for two reasons: first, the particles are larger (20 nm of γ -alumina particle vs 2 nm of 2-line ferrihydrite), so that less surface area is exposed to the X-ray beam for a given exposed volume. Second, Al has only one-half the scattering power of Fe (Z of 13 vs 26). Accordingly, signal-to-noise is much lower, reducing the amount of information that can be generated from the d-PDF in practice. From this, it can be deduced that there are three criteria that contribute to an optimal d-PDF experiment: (1) large specific surface area, (2) high scattering power of the atoms involved, and (3) a high surface loading of the adsorbed species (e.g., no signal was observed from a sample exposed to a 0.1 mM arsenate solution). As EXAFS suffers less from potential problems 1 and 3 and d-PDF has the potential to show correlations to higher r value, a combination of these techniques will be a good strategy to investigate environmental interfacial phenomena.

ASSOCIATED CONTENT

S Supporting Information. Detailed descriptions are available on EXAFS analysis and fitting results, quantum chemical calculations, characterization of γ -alumina, comparison of differential PDFs obtained at different Q_{max} values, and comparison of sorption capacities of various sorbants. This material is available free of charge via the Internet at <http://pubs.acs.org>.

AUTHOR INFORMATION

Corresponding Author

*E-mail: weili@udel.edu (W.L.); Richard.Harrington81@gmail.com (R.H.); ytang@seas.harvard.edu (Y.T.).

Present Addresses

¹Environmental Soil Chemistry Group, Delaware Environmental Institute, University of Delaware, Newark, DE, 19716, USA.

²School of Engineering and Applied Sciences, Harvard University, Cambridge, MA, 02318, USA.

³Department of Mechanical Engineering, Stanford University, Stanford CA, 94305, USA.

ACKNOWLEDGMENT

We sincerely appreciate three anonymous reviewers for their helpful comments. We thank Dr. Douglas B. Hausner for collecting the TEM images, Dr. Henry Pinto for supplying the structure file for the γ - Al_2O_3 crystal, and Dr. Wenqian Xu for discussions on the difference between EXAFS and d-PDF. Work done at

Argonne and use of the Advanced Photon Source was supported by the U.S. Department of Energy, Office of Science, Office of Basic Energy Sciences, under Contract No. DE-AC02-06CH11357. Financial support was provided by the National Science Foundation (NSF) through Collaborative Research in Chemistry (CRC), Grants CHE0714183 and CHE0714173.

REFERENCES

- (1) Sparks, D. L. *Environmental Soil Chemistry*, 2nd ed.; Academic Press: Boston, 2002.
- (2) Brown, G. E., Jr.; Parks, G. A. Sorption of trace elements from aqueous media: Modern perspectives from spectroscopic studies and comments on adsorption in the marine environment. *Int. Geol. Rev.* **2001**, *43*, 963–1073.
- (3) Ginder-Vogel, M.; Sparks, D. L. The impacts of X-ray absorption spectroscopy on understanding soil processes and reaction mechanisms. In *Developments in Soil Science 34: Synchrotron-based Techniques in Soils and Sediments*; Singh, B., Grafe, M., Eds.; Elsevier: Burlington, 2010; pp 1.
- (4) Egami, T.; Billinge, S. J. L. *Underneath the Bragg peaks: Structural analysis of complex materials*; Pergamon Press/ Elsevier: Oxford, 2003.
- (5) Billinge, S. J. L.; Kanatzidis, M. G. Beyond crystallography: the study of disorder, nanocrystallinity and crystallographically challenged materials with pair distribution functions. *Chem. Commun.* **2004**, 749–760.
- (6) Petkov, V. Nanostructure by high-energy X-ray diffraction. *Mater. Today* **2008**, *11*, 28–38.
- (7) Harrington, R.; Neder, R. B.; Parise, J. B. The nature of X-ray scattering from geo-nanoparticles: practical considerations of the use of the Debye equation and the pair distribution function for structure analysis. *Chem. Geol.*, doi:10.1016/j.chemgeo.2011.06.010.
- (8) Proffen, T.; Page, K. L. Obtaining structural information from the atomic pair distribution function. *Z. Kristallogr.* **2004**, *219*, 130–135.
- (9) Proffen, T.; Kim, H. Advances in total scattering analysis. *J. Mater. Chem.* **2009**, *19*, 5078–5088.
- (10) Chapman, K. W.; Chupas, P. J.; Maxey, E. R.; Richardson, J. W. Direct observation of adsorbed H₂-framework interactions in the Prussian Blue analogue Mn^{II}[Co^{III}(CN)₆]₂: The relative importance of accessible coordination sites and van der Waals interactions. *Chem. Commun.* **2006**, 4013–4015.
- (11) Chapman, K. W.; Chupas, P. J.; Kepert, C. J. Selective recovery of dynamic guest structure in a nanoporous Prussian Blue through in situ X-ray diffraction: A differential pair distribution function analysis. *J. Am. Chem. Soc.* **2005**, *127*, 11232–11233.
- (12) Kramer, M. J. A strategy for rapid analysis of the variations in the reduced distribution function of liquid metals and metallic glasses. *J. Appl. Crystallogr.* **2007**, *40*, 77–86.
- (13) Chupas, P. J.; Chapman, K. W.; Jennings, G.; Lee, P. L.; Grey, C. P. Watching nanoparticles grow: The mechanism and kinetics for the formation of TiO₂-supported platinum nanoparticles. *J. Am. Chem. Soc.* **2007**, *129*, 13822–13824.
- (14) Chupas, P. J.; Chapman, K. W.; Chen, H.; Grey, C. P. Application of high-energy X-rays and pair-distribution-function analysis to nano-scale structural studies in catalysis. *Catal. Today* **2009**, *145*, 213–219.
- (15) Waychunas, G. A.; Fuller, C. C.; Rea, B. A.; Davis, J. A. Wide angle X-ray scattering (WAXS) study of 'two-line' ferrihydrite structure: effect of arsenate sorption and counterion variation and comparison with EXAFS results. *Geochim. Cosmochim. Acta* **1996**, *60*, 1765–1781.
- (16) Harrington, R.; Hausner, D. B.; Bhandari, N.; Strongin, D. R.; Chapman, K. W.; Chupas, P. J.; Middlemiss, D. S.; Grey, C. P.; Parise, J. B. Investigations of surface structures by powder diffraction: a differential pair distribution function study on arsenate sorption on ferrihydrite. *Inorg. Chem.* **2010**, *49*, 325–330.
- (17) Michel, F. M.; Ehm, L.; Antao, S. M.; Lee, P. L.; Chupas, P. J.; Li, G.; Strongin, D. R.; Schoonen, M. A. A.; Phillips, B. L.; Parise, J. B. The structure of ferrihydrite, a nanocrystalline material. *Science* **2007**, *316*, 1726–1729.
- (18) Xu, W.; Hausner, D. B.; Harrington, R.; Lee, P. L.; Strongin, D. R.; Parise, J. B. Structural water in ferrihydrite and constraints this provides on possible structure models. *Am. Mineral.* **2011**, *96*, 513–520.
- (19) Waychunas, G. A.; Rea, B. A.; Fuller, C. C.; Davis, J. A. Surface chemistry of ferrihydrite: Part I. EXAFS studies of the geometry of coprecipitated and adsorbed arsenate. *Geochim. Cosmochim. Acta* **1993**, *57*, 2251–2269.
- (20) Sherman, D. M.; Randall, S. R. Surface complexation of arsenic(V) to iron(III) (hydr)oxides: Structural mechanism from ab initio molecular geometries and EXAFS spectroscopy. *Geochim. Cosmochim. Acta* **2003**, *67*, 4223–4230.
- (21) Huang, C. P.; Stumm, W. Specific adsorption of cations on hydrous γ -Al₂O₃. *J. Colloid Interface Sci.* **1973**, *43*, 409–420.
- (22) Arai, Y.; Elzinga, E. J.; Sparks, D. L. X-ray absorption spectroscopic investigation of arsenite and arsenate adsorption at the aluminum oxide-water interface. *J. Colloid Interface Sci.* **2001**, *235*, 80–88.
- (23) Strawn, D. G.; Scheidegger, A. M.; Sparks, D. L. Kinetics and mechanisms of Pb(II) sorption and desorption at the aluminum oxide-water interface. *Environ. Sci. Technol.* **1998**, *32*, 2596–2601.
- (24) Fitts, J. P.; Brown, G. E., Jr.; Parks, G. A. Structural evolution of Cr(III) polymeric species at the γ -Al₂O₃-water interface. *Environ. Sci. Technol.* **2000**, *34*, 5122–5128.
- (25) Tang, Y.; Reeder, R. J. Enhanced uranium sorption on aluminum oxide pretreated with arsenate. Part I: batch uptake behavior. *Environ. Sci. Technol.* **2009**, *43*, 4446–4451.
- (26) Chupas, P. J.; Qiu, X.; Hanson, J. C.; Lee, P. L.; Gery, C. P.; Billinge, S. J. L. Rapid-acquisition pair distribution function (RA-PDF) analysis. *J. Appl. Crystallogr.* **2003**, *36*, 1342–1347.
- (27) Chupas, P. J.; Chapman, K. W.; Lee, P. L. Applications of an amorphous silicon-based area detector for high-resolution, high-sensitivity and fast time-resolved pair distribution function measurements. *J. Appl. Crystallogr.* **2007**, *40*, 463–470.
- (28) Hammersley, A. P.; Svenson, S. O.; Hanfland, M.; Hauserman, D. Two-dimensional detector software: from real detector to idealised image or two-theta scan. *High Pressure Res.* **1996**, *14*, 235–248.
- (29) Qui, X.; Thompson, J. W.; Billinge, S. J. L. PDFgetX2: a GUI-driven program to obtain the pair distribution function from X-ray powder diffraction data. *J. Appl. Crystallogr.* **2004**, *37*, 678.
- (30) Sun, M.; Nelson, A. E.; Adjaye, J. Examination of spinel and nonspinel structural models for γ -Al₂O₃ by DFT and Rietveld refinement simulations. *J. Phys. Chem. B* **2006**, *110*, 2310–2317.
- (31) Mohan, D.; Pittman, C. U., Jr. Arsenic removal from water/wastewater using adsorbents—A critical review. *J. Hazard. Mater.* **2007**, *142*, 1–53.
- (32) Makris, K. C.; Sarkar, D.; Parsons, J. G.; Datta, R.; Gardea-Torresdey, J. L. X-ray absorption spectroscopy as a tool investigating arsenic(III) and arsenic(V) sorption by an aluminum-based drinking-water treatment residual. *J. Hazard. Mater.* **2009**, *171*, 980–986.
- (33) Stumm, W.; Morgan, J. J. *Aquatic Chemistry: Chemical equilibria and rates in natural waters*, 3rd ed.; John Wiley & Sons: New York, 1996.
- (34) Pinto, H. P.; Nieminen, R. M.; Elliott, S. D. Ab initio study of γ -Al₂O₃ surfaces. *Phys. Rev. B* **2004**, *70* (12), 125402-1–125402-11.
- (35) Ladeira, A. C. Q.; Ciminelli, V. S. T.; Duarte, H. A.; Alves, M. C. M.; Ramos, A. Y. Mechanism of anion retention from EXAFS and density functional calculations: Arsenic (V) adsorbed on gibbsite. *Geochim. Cosmochim. Acta* **2001**, *65*, 1211–1217.
- (36) Beaulieu, B. T.; Savage, K. S. Arsenate adsorption structures on aluminum oxide and phyllosilicate mineral surfaces in smelter-impacted soils. *Environ. Sci. Technol.* **2005**, *39*, 3571–3579.
- (37) Rehr, J. J.; Albers, R. C. Theoretical approaches to X-ray absorption fine structure. *Rev. Mod. Phys.* **2000**, *72*, 621–654.